Parametric design study of the Orbiting Astronomical Satellite for Investigating Stellar Systems (OASIS) space telescope

Siddhartha Sirsi*[a,b], Yuzuru Takashima[b], Art Palisoc[c], Aman Chandra[a], Chistopher Walker[a,b], Daewook Kim[a,b,d]

[a]Department of Astronomy and Steward Observatory, University of Arizona, 933 N. Cherry Ave., Tucson, AZ 85721, USA

[b]Wyant College of Optical Sciences, University of Arizona, 1630 E. University Blvd., Tucson, AZ 85721, USA

[c]L'Garde, Inc., 15181 Woodlawn Avenue, Tustin, CA 92780, USA

[d]Large Binocular Telescope Observatory, University of Arizona 933 N Cherry Avenue, Tucson, AZ 85721, USA

ABSTRACT

OASIS (Orbiting Astronomical Satellite for Investigating Stellar Systems) is a space-based observatory with a large inflatable primary reflector that will perform high spectral resolution observations at terahertz frequencies. An inflatable metallized polymer membrane serves as the primary antenna with large photon collecting area, followed by aberration correction mirror pair that enables a large field of regards of 0.1 degrees while achieving diffraction limited performance over a wide terahertz wavelength ranging from 80 μm to 660 μm. An analytical model is developed to define a solution space based on the profile of primary reflector which is a function of pressure. The photon collecting area, size and weight of the correction mirror pair, and optical aberrations are governed by a 1st order power arrangement of the telescope and is a function of base radius and clear aperture of the primary reflector. Based on the parametric design study, the figure of merit for the profile of the primary reflector is discussed and a baseline design satisfying the scientific and system requirements is proposed.

Keywords: OASIS mission, inflatable optics, solution space, terahertz astronomy

1. INTRODUCTION

In this paper the science goals[1] and system architecture[2] requirements that drives the design study are briefly discussed followed by iterative analytical model. Two cases for the primary reflector A1; Hencky[3] and paraboloid are investigated. A1 figure of merit based off parametric design study is discussed. Solution space considering the A1 profile, clear aperture, and sensitivity to system tolerances is produced and the performance of a baseline design satisfying all the requirements is presented.

1.1 Science goals and system architecture requirements

OASIS aims to have a collecting area 20 times greater[1] than that of Herschel Space Observatory[4]. Since OASIS is a MidEx mission concept with a mass cap of 1700 kg, to achieve the proposed collecting area, a system architecture with 13 kg/m^2 is required[2]. The requirements driving the parametric study are listed in Table 1. The receiver band wavelength definitions required to generate solution space plots are listed in Table 2.

Table 1. OASIS science goals and system architecture requirements.

Collecting area	>120 m^2
Field of view	3 arcmin (radius)
Mass/Collecting area	13 kg/m^2
Wavelength	660 μm to 80 μm

Table 2. OASIS receiver band wavelength definition[1].

Band 1	658.88 μm to 521.38 μm
Band 2	272.54 μm to 136.27 μm
Band 3	121.13 μm to 104.28 μm
Band 4	81.42 μm to 81.2 μm
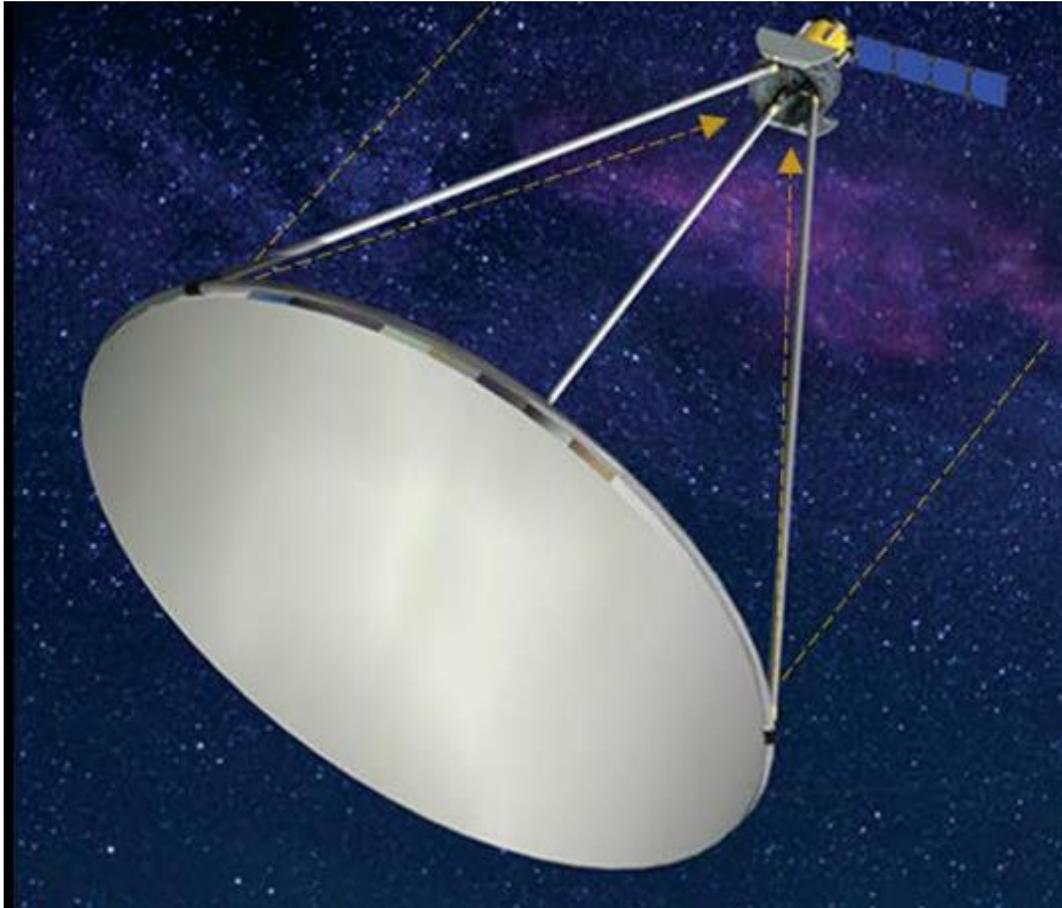
Figure 1. OASIS concept showing the deployed configuration.

2. METHODOLOGY

OASIS optical design offers a unique challenge since the primary mirror or antenna (A1) is an inflatable membrane and its surface profile varies w.r.t pressure. The goal is to determine the best suitable design which meets all the science goals and system architecture requirements listed in Table 1. A parametric design study in which the surface profile and the entrance pupil diameter of A1 are varied is required to achieve this goal.

2.1 Iterative Analytical Model

An iterative analytical model is developed to determine the location and size of secondary optics, and the geometrical collecting area of the telescope system for different combinations of A1 surface profiles and apertures
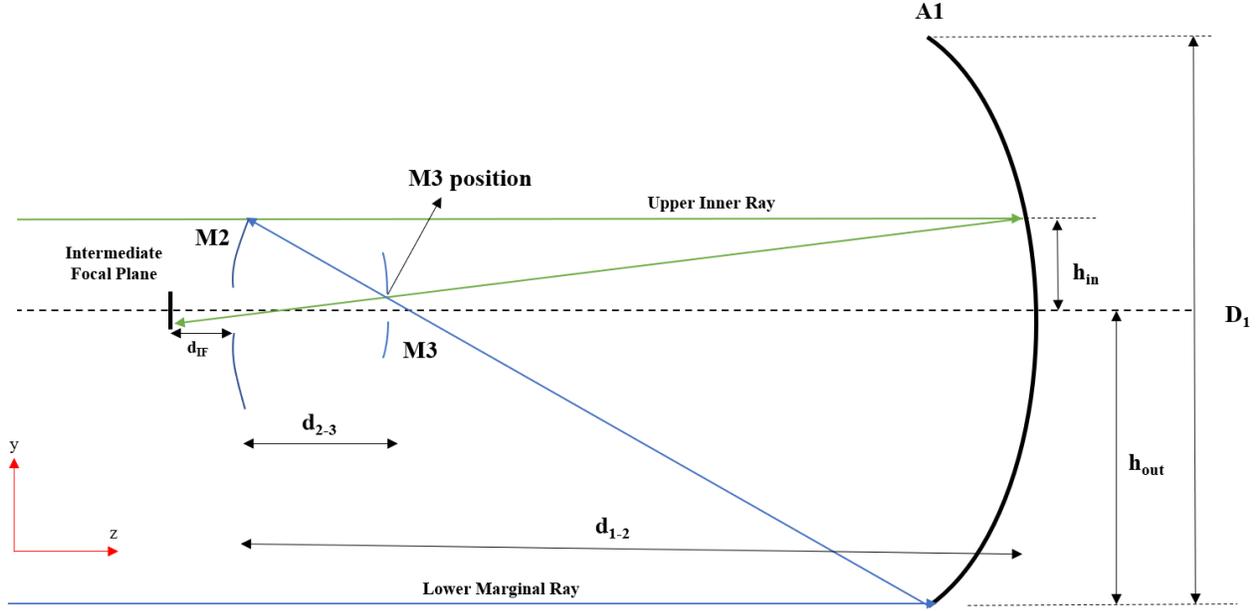
Figure 2. Analytical model showing the ray trace used to determine the position and size of secondary optics (M2 and M3)

Step 1: Given the surface profile and the entrance pupil diameter (D_1) of A1, and the field of view (θ), the M2 hole diameter (H_{M2}) is estimated.

$$H_{M2} = 2\tan(\theta)d_{1-2} + \frac{d_{IF}}{(f/\#)_{sys}} \tag{1}$$

$d_{1-2} = \dfrac{R_1}{2}$ where R_1 is the base radius of curvature of A1.

Step 2: The height of the incident ray (shown as Upper Inner Ray in Figure 1) at A1 (h_{in}) which results in the image height equal to $H_{M2}/2$ at the initial intermediate focal plane is calculated. $h_{out} = D_1/2$ is the height of the marginal ray at A1 (shown as Lower Marginal Ray in Figure 1).

Step 3: The intersection of the Upper Inner Ray and the Lower Marginal Ray determines the location of M3 and its hole size (H_{M3}).

Step 4: Given the distance d_{2-3} between M2 and M3, the location of M2 is updated.

Step 5: The height of the lower marginal ray at the updated location of M2 determines the diameter of M2 (D_{M2}).

Step 6: Diameter of M3 (D_{M3}) is calculated by equating the $(f/\#)_{sys}$ with $(f/\#)_{M3}$.

$$(f/\#)_{sys} = \frac{(R_1/2)}{2h_{out}} \tag{2}$$

$$(f/\#)_{M3} = \frac{d_{2-3} + d_{IF}}{D_{M3}} \tag{3}$$

$$D_{M3} = (d_{2-3} + d_{IF})\frac{2h_{out}}{R_1/2} \tag{4}$$

Step 7: Geometrical collecting area (CA_{Geo}) of the system is calculated.

$$CA_{Geo} = \left(h_{out}^2 - h_{in}^2 \right) \pi \tag{5}$$

The above steps are iterated till h_{in} value converges.

2.2 Effective Collecting Area

The output of iterative analytical model is used to develop ZEMAX models. The RMS wavefront error (σ) is employed as a figure of merit to evaluate the performance of the different configurations and calculate the effective collecting area. The system RMS wavefront error (σ_{sys}) w.r.t to decenter in x, y, and z directions, tilt about x and y axes of individual optical elements is given by

$$\sigma_{sys} = \sqrt{\sigma_{M1}^2 + \sigma_{M2}^2 + \sigma_{M3}^2 + \sigma_{Baseline}^2} \tag{6}$$

Where the RMS wavefront error due to perturbation of individual optical elements is given by

$$\sigma_{element} = \sqrt{\sigma_{Dec\_x}^2 + \sigma_{Dec\_y}^2 + \sigma_{Dec\_z}^2 + \sigma_{Tilt\_x}^2 + \sigma_{Tilt\_y}^2} \tag{7}$$

Effective collecting area is a function of geometrical collecting area and area averaged Strehl intensity ratio. The Strehl intensity ratio (SIR) can be approximated as[5]

$$SIR = e^{-\left(2\pi \frac{\sigma}{\lambda}\right)^2} \tag{8}$$

$\sigma =$ RMS Wavefront Error (μm)

$\lambda =$ Wavelength (μm)

Assuming σ varies quadratically with normalized field of view (r)

$$\sigma(r) = \left(\sigma_{off-axis} - \sigma_{on-axis} \right) r^2 + \sigma_{on-axis} \tag{9}$$

Area averaged SIR is given by

$$SIR(r) = 2\int_0^1 r e^{-\left(2\pi \frac{\left(\sigma_{off-axis} - \sigma_{on-axis}\right) r^2 + \sigma_{on-axis}}{\lambda}\right)^2} dr \tag{10}$$

Effective collecting area of the system is then calculated as

$$EA(r) = 2 \times Area \int_0^1 r e^{-\left(2\pi \frac{\left(\sigma_{sys\,off-axis} - \sigma_{sys\,on-axis}\right) r^2 + \sigma_{sys\,on-axis}}{\lambda}\right)^2} dr \tag{11}$$

Starting with the profile of A1, entrance pupil diameter, and FOV, the parameters of the secondary optical elements are determined. Effective collecting area is then calculated using the geometrical collecting area and the area averaged Strehl intensity ratio. These results are used to generate solution space contour plots which will aid in the selection of a suitable design which meets all the science requirements and is within the defined system constraints. In the following section, the performance and feasibility of different A1 profiles are investigated using the methodology laid out in this section.

3. CASES

3.1 Hencky Surface

An inflatable mirror formed by using two thin, circular, monolithic flat polymer membranes will result in a surface profile which is neither spherical nor parabolic, but an oblate spheroid expressed by an even power series known as Hecky Curve[3].

$$z(u) = \frac{D}{64F^2}\left(u^2 + 0.1111u^4\right) \tag{12}$$

where D is the diameter of the mirror, F is the $f/\#$, and u is the fractional radial distance from the center of membrane.

Iterative analytical model is run using the following parameters:

$R_1 = 50$ m
$D_1 = [12$ m 13 m 14 m 15 m 16 m 17 m 18 m 19 m 20 m$]$
$d_{2-3} = 2.2$ m
$d_{IF} = 200$ mm
$\theta = \pm0.05°$ and $\lambda = 111$ μm

The results of the parametric sweep of D_1 for $R_1 = 50$ m and its comparison with the optimized ZEMAX models are listed in Table 3.

Table 3. Parametric sweep of D_1 for $R_1 = 50$ m and its comparison with the optimized ZEMAX models.

D_1 (m)	d_{1-2} (m)	D_{M2} (m)	H_{M2} (mm)	D_{M3} (m)	H_{M3} (mm)	Analytical Geometric Collecting Area (m²)	ZEMAX Geometric Collecting Area (m²)
12	25.7705	1.33	141	1.15	134	102.55	100.31
13	25.5295	1.52	149	1.24	208	116.62	116.3
14	25.2675	1.74	156	1.34	301	129.62	129.21
15	24.9872	1.97	164	1.44	410	141.49	140.91
16	24.6881	2.23	171	1.53	533	152.29	151.72
17	24.3737	2.51	179	1.63	665	162.61	161.67
18	24.0431	2.80	186	1.72	810	172.20	171.13
19	23.6986	3.12	194	1.82	965	181.59	181.20

D1 = Entrance pupil diameter of A1
d_{1-2} = Distance between A1 and M2
D_{M2} = Diameter of M2
H_{M2} = Hole diameter of M2
D_{M3} = Diameter of M3
H_{M3} = Hole Diameter of M3

The analytical model is in close accordance with the optimized ZEMAX model. Table 1 shows that the Iterative Analytical Model developed in the previous section can be used to accurately predict the optical design parameters without having to go through the entire design process using ray tracing software.

Hencky surface profile for A1 results in very large M2 and M3 mirror sizes and does not meet the minimum photon collecting area as required by the science requirements. This is not a suitable surface profile, and no further analysis is required.

3.2 Paraboloid

Instead of forming the primary mirror from a flat membrane, several pre-formed slices of membranes (gores) can be stitched together to create the desired A1 profile upon inflation[6]. The goal is to define an A1 profile which minimizes the secondary optical element sizes while maximizing the photon collecting area. Keeping this in mind, a parabolic profile for A1 is investigated for the following parameters:

$R_1 = 50$ m

$D_1 = [12$ m 13 m 14 m 15 m 16 m 17 m 18 m 19 m 20 m$]$

$d_{2-3} = 0.5$ m

$d_{IF} = 100$ mm

$\theta = \pm 0.05°$ and $\lambda = 111$ μm

From the plots in Figure 2, it is clear that a parabolic A1 profile is best suited to achieve the above-mentioned goal. L'Garde Inc were tasked with investigating the feasibility of generating a parabolic A1 profile with radius of curvature of 50 m[6]. The data provided by L'Garde; nominal pressure, 10% lower, and 10% higher is fit to an 8th order polynomial to define the surface profile of A1 (Table 4).

Although this profile results in smaller M2 and M3 mirror sizes compared to Hencky surface, they are still larger than those resulting from a pure analytical parabolic shape (Figure 3). In the next section, the figure of merit for evaluating A1 profile is discussed and a baseline design is proposed.
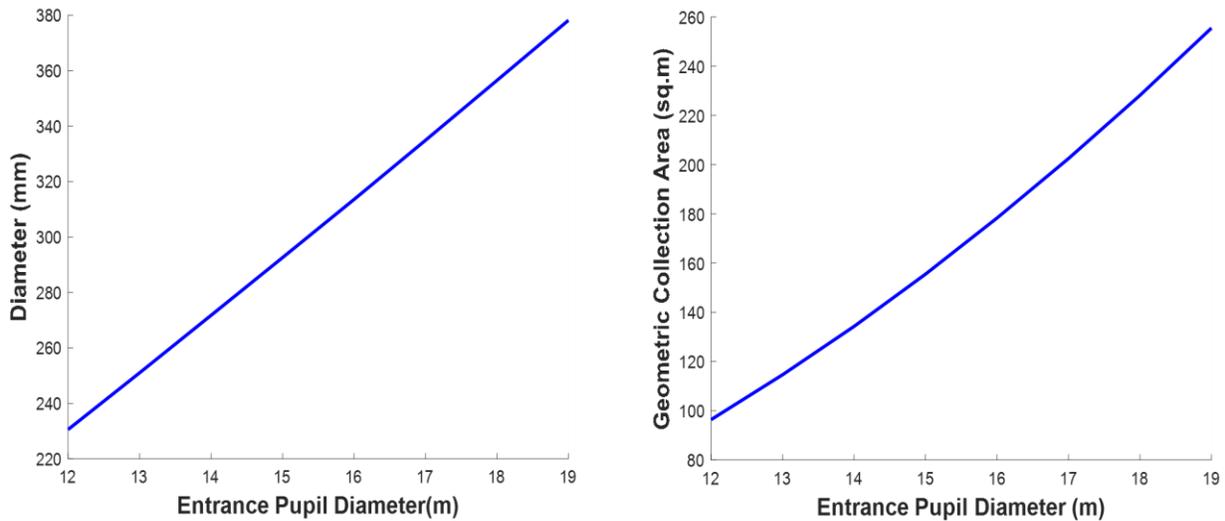
Figure 3. Plot of M2 and M3 diameters and geometric collecting area for a parabolic A1 wirh $R_1 = 50$ m as a function of D_1.

Table 4. L'Garde Inc data for generating a parabolic A1 profile with R_1= 50 m and D_1= 20 m fit to 8th order polynomial.

Pressure	Aspheric Coefficients				Base Radius (m)
	A2	**A4**	**A6**	**A8**	
10% Low	9.9711e-6	1.9272e-15	3.7815e-23	7.3647e-32	50.14
Nominal	9.9865e-6	1.8699e-15	4.1282e-23	6.5595e-32	50.06
10% High	1.0009e-5	1.3386e-15	3.3389e-23	4.0683e-32	49.95
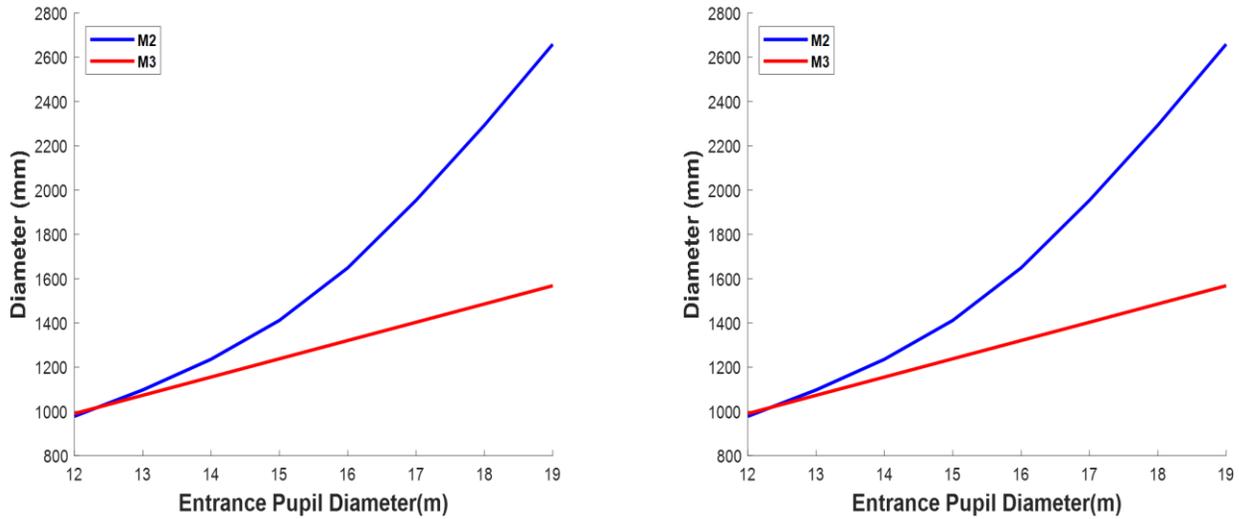
Figure 4. Plot of M2 and M3 diameters and geometric collecting area for nominal pressure A1 profile provided by L'Garde Inc for R_1= 50 m as a function of entrance pupil diameter D_1.

4. DISCUSSION

4.1 A1 Figure of Merit

The data from L'Garde Inc for a parabolic A1 profile with base radius of curvature of 50 m at nominal pressure is further analyzed to define the figure of merit for evaluating A1 profile performance. This profile, P1 is decomposed to result in a best fit parabola and the residual W-curve (Figure 4). The W-curve is fit to an 8th order polynomial and transverse ray analysis is carried out to identify the individual contribution of aspheric coefficients to the overall aberration induced by A1.

Total aberration induced by P1 is equal to the combination of defocus (w_{020}) , aberration induced by 4th order term of W-curve (w_{040}) , and aberration induced by 6th order term of W-curve (w_{060}). 8th order term is neglected as its contribution to the overall aberration is small compared to the other terms.
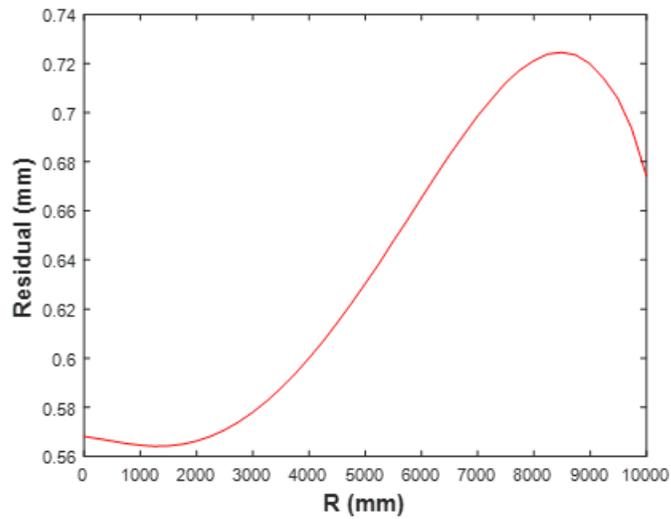
Figure 5. W- Curve: L'Garde data for parabolic A1 profile id fit to parabola with base radius of 50033.53 mm and the residual is plotted as a function of radial distance.

$$\varepsilon_y = -2 \times f/\# \times \left(2w_{020}\rho^2 + 4w_{040}\rho^4 + 6w_{060}\rho^6\right) \tag{13}$$

From transverse ray analysis, $\varepsilon_y = 671.3$ mm, $w_{040} = 10.4$ mm, $w_{060} = 12.9$ mm and $f/\# = 1.6$. Substituting in Eq (13)

$$w_{020} = 164.4 \text{ mm}$$

Defocus affects the location of mirrors and can be accounted for during the design process. The spherical aberration terms w_{040} and w_{060} affect the size of secondary mirror sizes. Reduction in the contribution of these two terms results in smaller secondary mirror sizes. A scaling factor is applied to A4 and A6 aspheric terms to demonstrate its effect on M2 and M3 sizes (Table 5). The peak to valley error w.r.t the best fit parabola can then be used a figure of merit to evaluate the performance of A1.

Table 5. Variation of M2 diameter as a function of scaling factor applied to A4 and A6 aspheric coefficients of W-curve. P-V error w.r.t best fit parabola as a figure of merit for evaluating A1 performance.

Scaling Factor	A4	A6	M2 Diameter (mm)	Peak to valley error w.r.t best fit parabola (mm)
1	1.87e-15	4.128e-23	1322	13.53
0.5	9.349e-16	2.064e-23	592	6.9
0.1	1.87e-16	4.128e-24	456	1.6
0.01	1.87e-17	4.128e-25	370	0.4

4.2 Baseline Design

In order to test the robustness of the definition of A1 figure of merit, L'Garde Inc data for A1 parabolic profile, P2 for R_1 = 50 m, D_1 = 20 m at 20% lower than nominal pressure is analyzed. The total aberration induced by A1 is now 147.3 mm as compared to 671.3 mm for the nominal pressure case. This profile P2 falls right in the middle of Table 5 between 0.5 and 0.1 scaling factor condition. A scaling factor of 0.15 corresponds closely with the profile P2. Thus, the definition of A1 figure of merit holds under scrutiny and the scaling factor of 0.15 can be used to approximate the A1 profiles for conducting the complete parametric design analysis.

L'Garde Inc data for 40 m, 50 m, and 60 m parabolic profile at nominal pressure are fit to an 8th order polynomial and the aspheric terms are scaled by 0.15 to get the desired A1 profiles. The following parameters are defined for the baseline design and the sensitivity analysis parameters are listed in Table 6.

R_1 = [40m 50m 60m]

D_1 = [15m 16m 17m 18m 19m]

$d_{2-3} = 0.7$ m

$d_{IF} = 100$ mm

$\theta = \pm 0.05°$

Table 6. Sensitivity analysis parameters

Optical Element	Parameter	
A1	Decenter X = 0.5 mm	Tilt X = 0.001 deg
	Decenter Y = 0.5 mm	Tilt Y = 0.001 deg
	Decenter Z= 0.5 mm	Tilt Z = 0 deg
M2	Decenter X = 0.1 mm	Tilt X = 0.001 deg
	Decenter Y = 0.1 mm	Tilt Y = 0.001 deg
	Decenter Z= 0.5 mm	Tilt Z = 0 deg
M3	Decenter X = 0.1 mm	Tilt X = 0.001 deg
	Decenter Y = 0.1 mm	Tilt Y = 0.001 deg
	Decenter Z= 0.5 mm	Tilt Z = 0 deg

The steps involved in the parametric design study are shown in Figure 5. The solution space contour plots for different wavelength bands are shown from Fig. 6 to Fig. 9. The solution space contour plots are a guide for selecting the best suitable combination of A1 profile and entrance pupil diameter which satisfies the science requirements and is within the system constraints. One of the solutions given by R_1 = 50 m and D_1 = 17 m is selected and its performance is analyzed using ZEMAX.

Table 7. Parametric design study result for A1 with R_1= 50 m and D_1= 17 m.

M2	Diameter = 0.6 m	Mass = 3.6 kg
M3	Diameter = 0.46 m	Mass = 2 kg
Band 1	Effective Collecting Area = 197.8 m^2	Aperture Efficiency = 0.87
Band 2	Effective Collecting Area = 189.74 m^2	Aperture Efficiency = 0.83
Band 3	Effective Collecting Area = 148.21 m^2	Aperture Efficiency = 0.65
Band 4	Effective Collecting Area = 113 m^2	Aperture Efficiency = 0.49
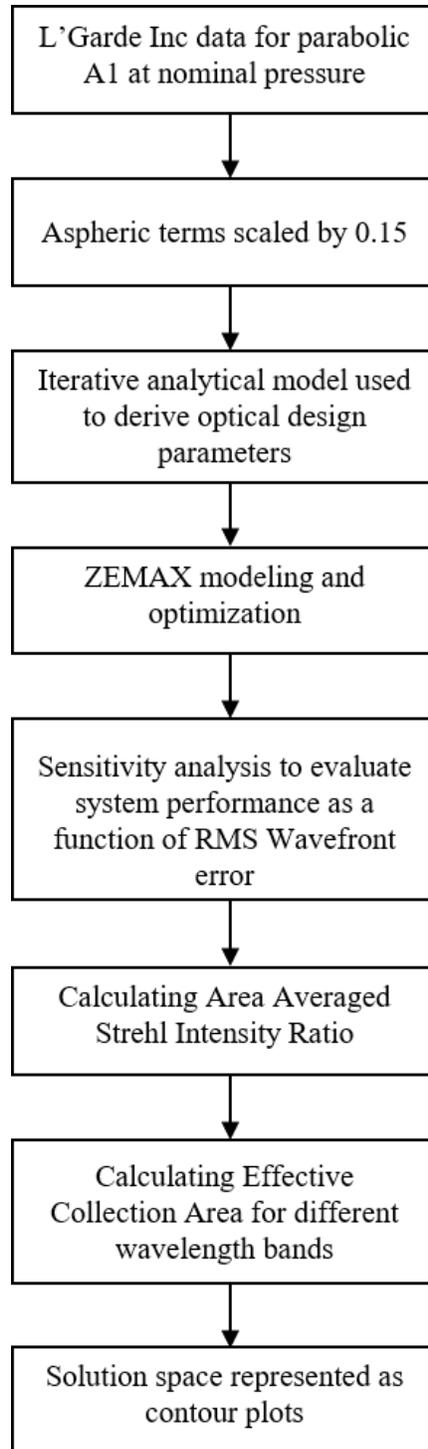
Figure 6. Steps involved in parametric design study.
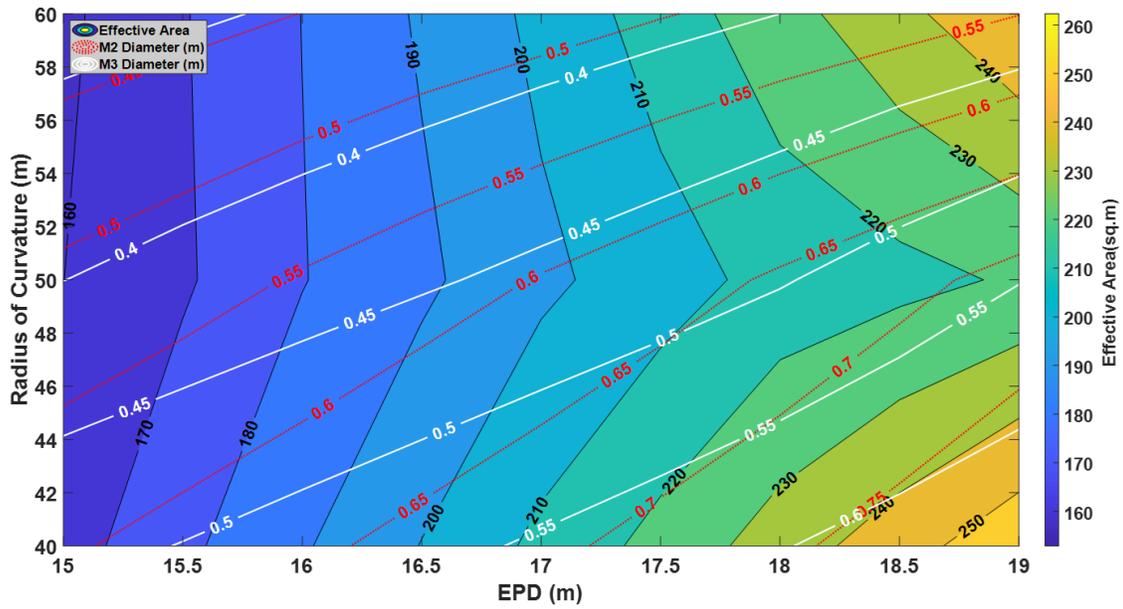
Figure 7. Solution space contour plot depicting effective collecting area, M2, and M3 diameter for Band 1.
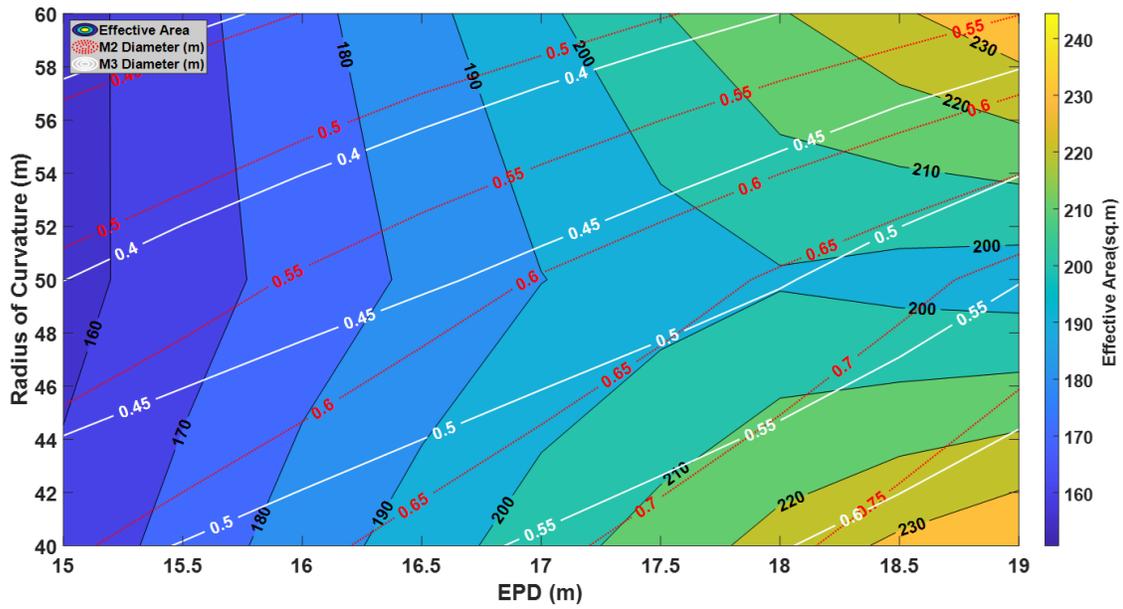
Figure 8. Solution space contour plot depicting effective collecting area, M2, and M3 diameter for Band 2.
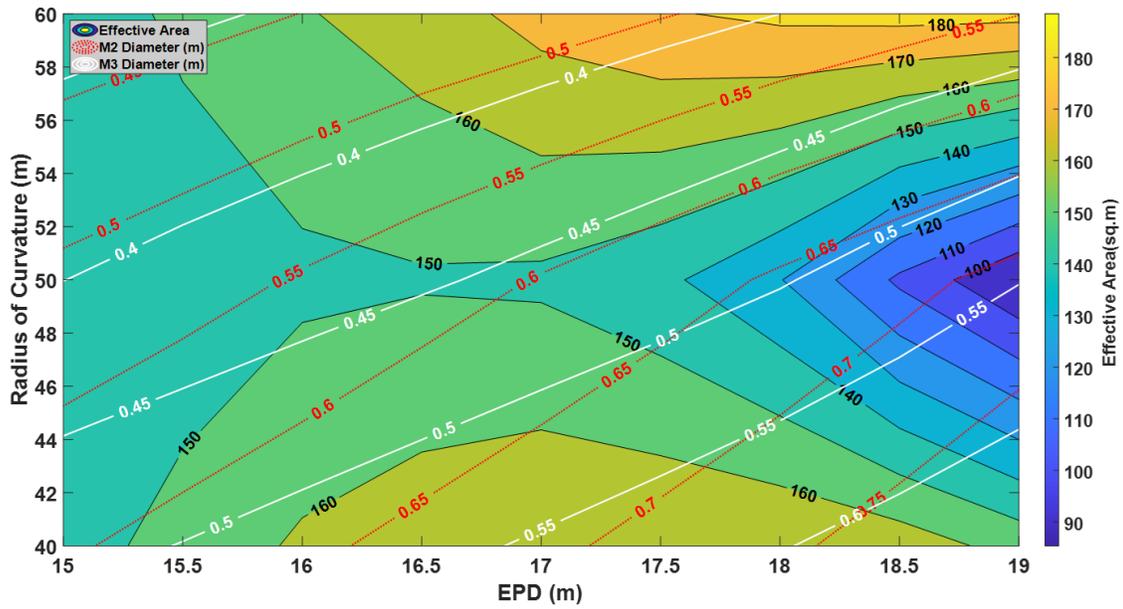
Figure 9. Solution space contour plot depicting effective collecting area, M2, and M3 diameter for Band 3.
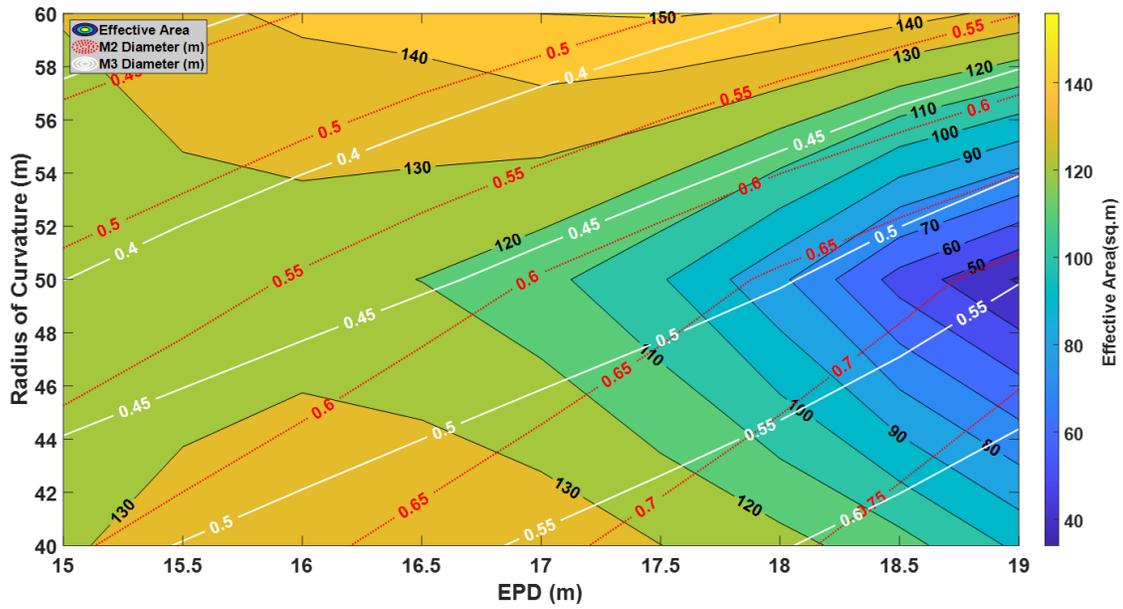
Figure 10. Solution space contour plot depicting effective collecting area, M2, and M3 diameter for Band 4.
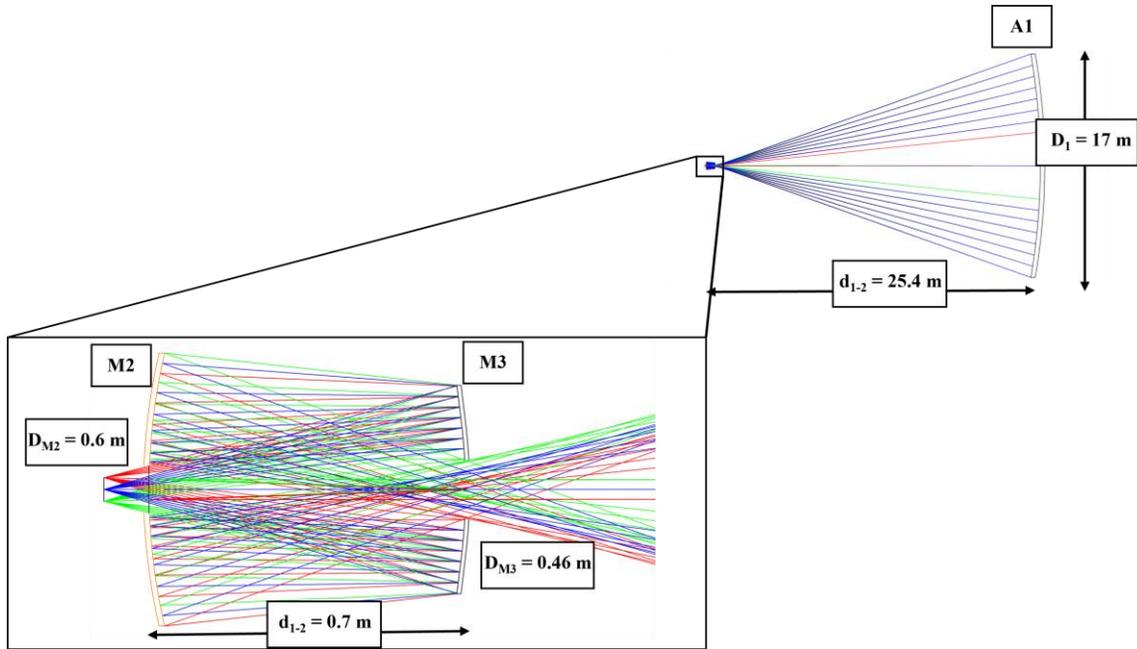
Figure 11. ZEMAX ray trace model for R_1= 50 m and D_1= 17 m.
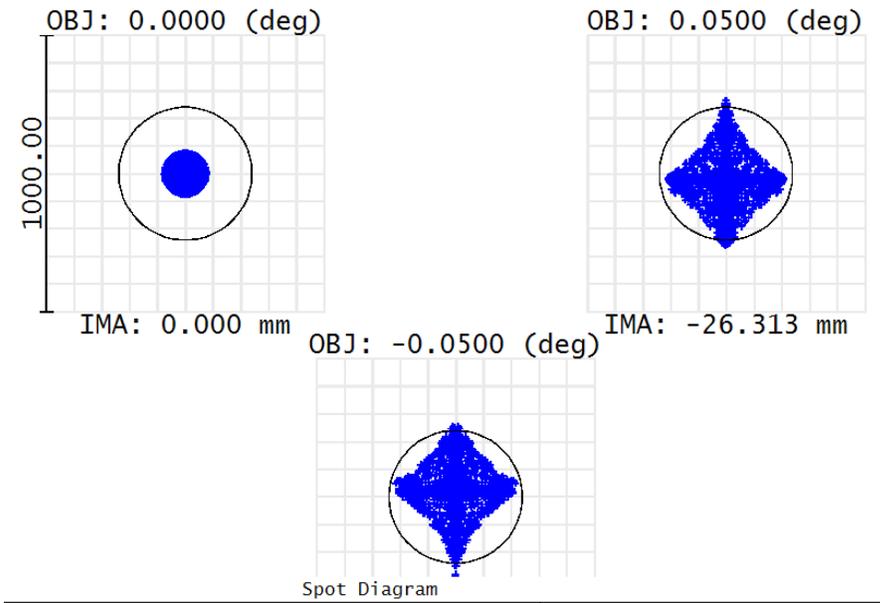
Figure 12. Spot diagram showing diffraction limited performance across the field of view.
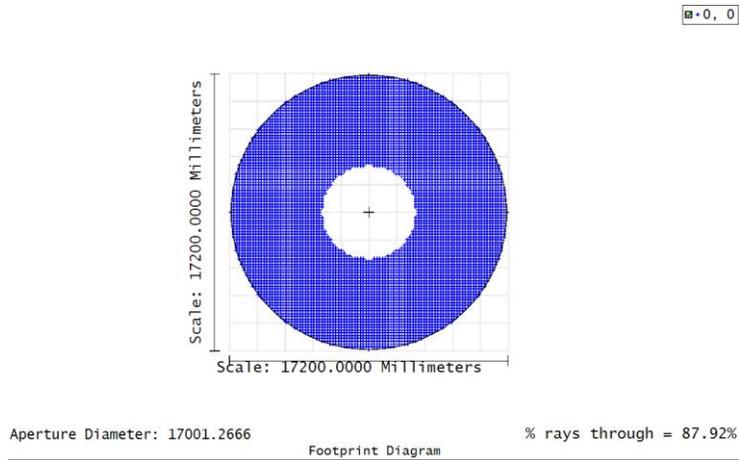
Figure 13. Footprint diagram showing percentage of unvignetted rays relative to A1. The geometric collecting area = 199.56 m^2.
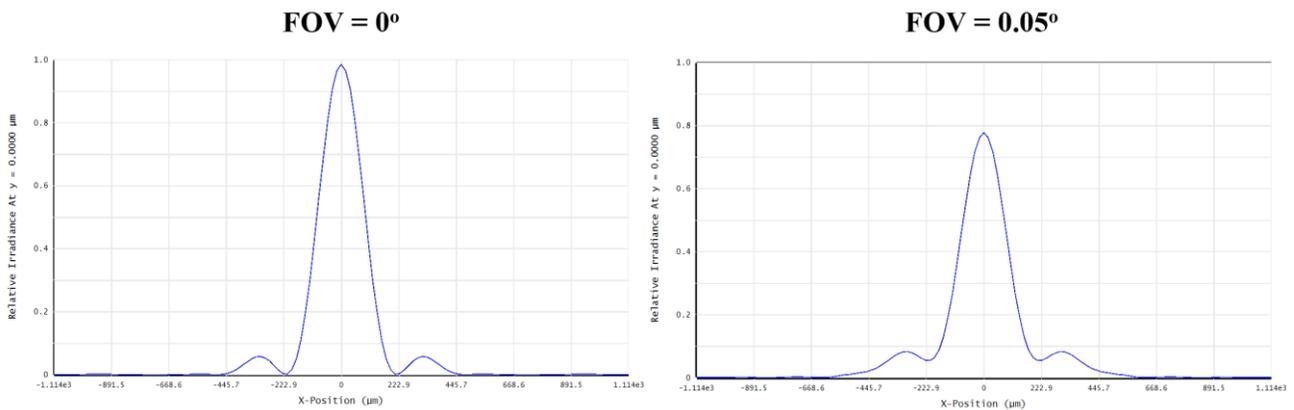
Figure 14. Point spread function at on-axis and off-axis positions.
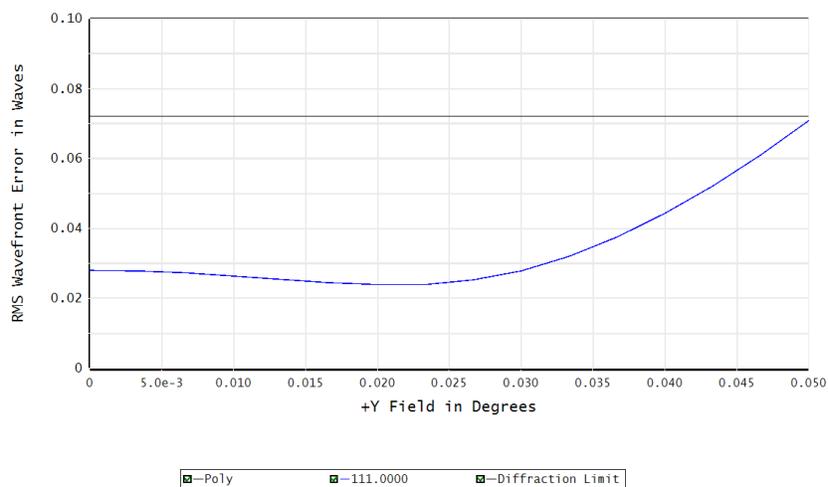
Figure 15. RMS wavefront error as a function of field of view at Band 3.

5. CONCLUSION

The unique challenges presented by the OASIS mission due to the inflatable primary reflector and the methodology used to solve them have been presented in this paper. The surface profile of the primary reflector is a function of pressure. In order to find the suitable profile which results in an optical design satisfying the science goals and system architecture requirements, an iterative analytical model is developed to perform parametric design study. Based off the parametric design study the figure of merit for the primary reflector is defined. The resulting solution space contour plots are then used to identify a baseline design satisfying all the requirements.

REFERENCES

[1] Christopher Walker, et al., "Orbiting Astronomical Satellite for Investigating Stellar Systems (OASIS) Following the Water Trail from the Interstellar Medium to Oceans," SPIE Paper #11820-26, Proc SPIE, Optics+Photonics, San Diego, California, 1-5 August 2021.

[2] Jonathan W. Arenberg, et al, "OASIS Architecture: Key Features", SPIE Paper #11820-31, Proc SPIE, Optics+Photonics, San Diego, California, 1-5 August 2021.

[3] A. B. Meinel and M. P. Meinel, "Inflatable membrane mirrors for optical passband imagery," *Opt. Eng.*, vol. 39, pp. 541–550, 2000, doi: 10.1117/1.602393

[4] G. L. Pilbratt *et al.*, "Herschel Space Observatory," *Astron. Astrophys.*, vol. 518, no. 7–8, 2010, doi: 10.1051/0004-6361/201014759

[5] Virendra N. Mahajan, "Strehl ratio for primary aberrations in terms of their aberration variance," J. Opt. Soc. Am. 73, 860-861 (1983)

[6] Arthur L. Palisoc, et al, "Analytical and finite element analysis tool for nonlinear membrane antenna modeling for astronomical applications", SPIE Paper #11820-32, Proc SPIE, Optics+Photonics, San Diego, California, 1-5 August 2021.